A Physical, Yet Simple, Small-Signal Equivalent Circuit for the Heterojunction Bipolar Transistor

Y. Gobert, P. J. Tasker, and K. H. Bachem

***Abstract*— A physical, yet simple, small-signal equivalent circuit for the heterojunction bipolar transistor (HBT) is proposed. This circuit was established by analyzing in detail the physical operation of the HBT. The model verification was carried out by comparison of the measured and simulated S- and Z-parameters for both passive (reverse-biased) and active bias conditions. A feature of this model is that it uses a direct extraction method to determine the parasitic elements, in particular, the parasitic capacitances. The excellent agreement between the measured and simulated parameters was verified all over the frequency range from 0.25 to 75 GHz.**

I. Introduction

The equivalent circuit of a transistor must be determined by considering its physical operation, particularly for high frequencies and/or the optimization of the performance of the transistor. In the case of the field-effect transistor FET (MESFET and HEMT) there is only one circuit commonly used [1], however there are two different equivalent circuits used for the bipolar transistors (BT's) (T-topology, π-topology) [2], [5] due to the two different physical approaches for modeling this transistor.

With the commonly used HBT equivalent circuits [2]–[5], even the one proposed by Costa [2], we found that the measured and computed Z-parameters do not agree well, especially at low frequencies, although the S-parameters appeared to be correct. Furthermore, the required values of some elements of the equivalent circuit were sensitive to the initial starting values, e.g., the access resistances $R_b,\ R_e,\ R_c$, the dc current gain, or even the pad parasitics. We also noticed that the fitted values of some intrinsic elements were sensitive to the initial starting values. These observations prompted us to reconsider not only the extraction but also the topology of the equivalent circuit. So, we investigated the HBT circuit topology to establish what had to be modified or/and improved in the previously published circuits.

Generally, the intrinsic device is modeled with a simple lumped-element circuit. As shown in Fig. 1(a) and (b), however, a number of RC distributed circuits are possibly required: one beneath the emitter and another between the base and the collector. Ignoring these distributed effects can limit the accuracy of the lumped-element circuit. As a consequence, but to keep the circuit as simple as possible, the RC distributed circuit appearing between the base and the collector was replaced by a simple π-RC circuit. That way, we derived a more physical equivalent small-signal circuit of the active HBT, as depicted on the Fig. 2, but also of the passive (reverse-biased) HBT $\{\beta = 0\}$.

To verify the validity of our resulting circuit, we then performed S-parameter measurements throughout the frequency range from 0.25 to 75 GHz by using an HP vector network analyzer. The values of the equivalent small-signal circuit elements were fitted by using the EEsof Touchstone program once the values of the parasitic elements had been assessed.

Manuscript received February 14, 1996; revised September 23, 1996. This work was supported by the European Community within the "Human Capital and Mobility" program.

The authors are with the Fraunhofer-Institut für Angewandte Festkörperphysik, D-79108 Freiburg, Germany.

Publisher Item Identifier S 0018-9480(97)00281-0.

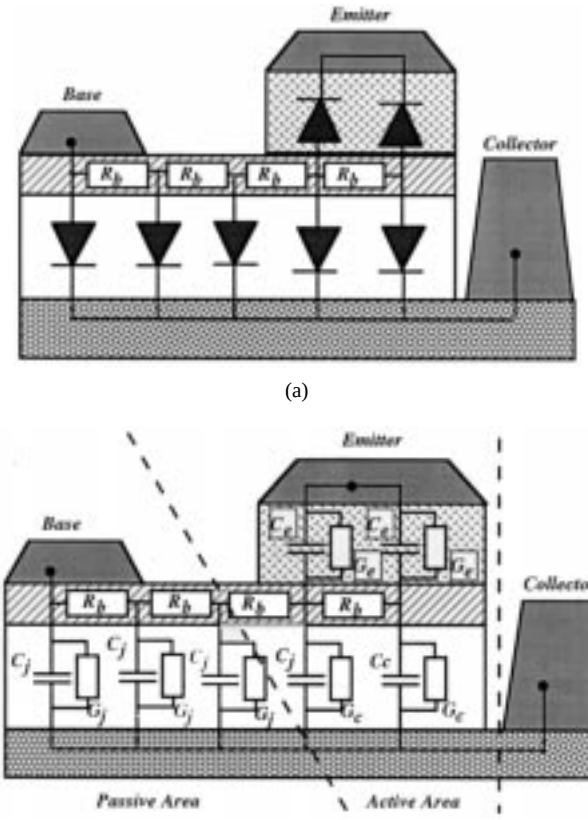

Fig. 1. (a) Sketch of the HBT cross section. (b) Resulting circuit.

All the transistors characterized were GaInP/GaAs hole-barrier-bipolar-transistors (HBBT's) with emitter areas from $1 * 20\ \mu\text{m}^2$ to $2.5 * 20\ \mu\text{m}^2$ [5]. The MOVPE-grown device layer structure consists of a 1500-Å GaAs emitter cap-layer doped n^+ $(7 \cdot 10^{18}\ \text{At/cm}^3)$, 1500-Å GaAs emitter layer doped n $(7 \cdot 10^{17}\ \text{At/cm}^3)$, 100-Å InGaP (NID), 1000-Å GaAs base layer doped p^+ $(6.5 \cdot 10^{19}\ \text{At/cm}^3)$, 5000-Å GaAs pre-collector layer doped n^- $(10^{16}\ \text{At/cm}^3)$, and 1500-Å GaAs collector layer doped n^+ $(7 \cdot 10^{18}\ \text{At/cm}^3)$. All of these layers were grown on a semi-insulating substrate.

Before investigating the validity and performing the extraction of the intrinsic equivalent circuit model, however, the values of the parasitics must be determined. By using a test structure, however, we had a strong disagreement between their measured and fitted values, more particularly the parasitic capacitances. This technique is inaccurate since, among other things, the fringing capacitances and the inductances induced along the "fingers" are ignored. Unfortunately up to now, no better solution has been proposed. So, we undertook a study to establish an direct extraction method for the parasitics useful for the HBT like the one available for the FET [1]. Then we validated it through experimental measurements.

II. Extraction of the Parasitic Elements

First of all, we focused on the extraction of the parasitic capacitances, which remains up to now the most difficult to obtain by measurements. On the other hand, techniques similar to those used for the FET have already been proposed to extract the inductances as well as the emitter and the collector access resistances [6], [8] directly from the DUT.

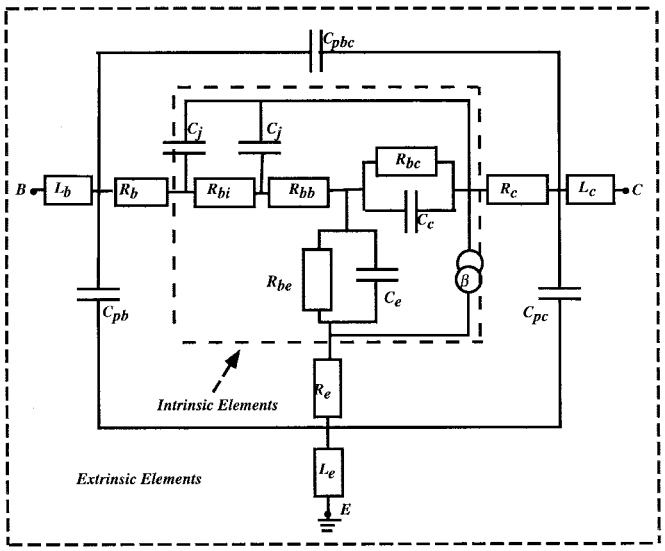

Fig. 2. Resulting equivalent circuit of the HBT when normally biased. When reverse-biased, $\beta = 0$.

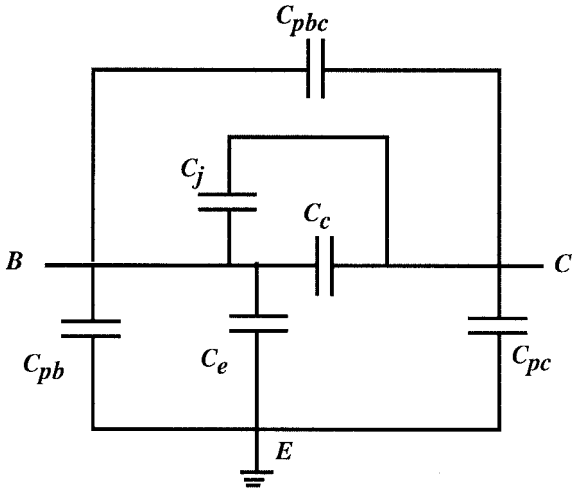

Fig. 3. HBT equivalent circuit when reverse-biased used to extract the parasitic capacitances.

A. Parasitic Capacitances

It has been already suggested to reverse-bias the HBT to estimate the values of the intrinsic capacitances [7], a method similar to the one proposed for the FET's by Dambrine [1], but without being able to extract directly from the measurement the parasitic capacitances. Thus, by analogy with Dambrine or Lee [1], [7], consider the simplified equivalent circuit of the HBT when reverse-biased (Fig. 3) valid as long as the influence of the inductances and resistances remains negligible, tour circuit has a simple π-topology, and it contains only capacitances. So, its Y-parameters are expressed simply as follows [see (1)]:

$$\begin{aligned} Y_1 &= j\cdot\omega\cdot C_{\rm in} & Y_{11} &= Y_1 + Y_2 \\ Y_2 &= j\cdot\omega\cdot C_{\rm bc} \quad \text{with} & Y_{12} &= Y_{21} = -Y_2 \\ Y_3 &= j\cdot\omega\cdot C_{\rm out} & Y_{22} &= Y_3 + Y_2 \end{aligned} \tag{1}$$

where $\{C_{\rm pb} + C_e\}$ equals $C_{\rm in}$, $\{C_{\rm pbc} + C_c + C_j\}$ equals $C_{\rm bc}$ and $C_{\rm pc}$ equals $C_{\rm out}$.

Now the problem consists of distinguishing the parasitic capacitances from the junction capacitances. In that case, an answer was given by the theory [5]. Indeed, the value of the junction capacitance $C_{\rm junct}$ due to the depletion region in an abrupt p-n junction is as follows as a function of the applied reverse voltage:

$$C_{\rm junct} = S\cdot\frac{k}{\sqrt{(\phi_b + V_a)}} \tag{2}$$

where S is the area of the junction, k is function of the acceptor and donor doping levels, ϕ_b is the built-in voltage, and V_a is the applied reverse voltage. So, by plotting the values of the input capacitance $C_{\rm in}$, the feedback capacitance $C_{\rm bc}$ and the output capacitance $C_{\rm out}$ versus the inverse of the square root of $\{\phi_b + V_a\}$, we may determine the values of the parasitic capacitances by extrapolating the resulting plots up to the ordinate $(V_a \to \infty)$ (see Fig. 5).

As shown in the Fig. 4, the theoretical expressions of the imaginary part of the Y_i [see (1)] predict well the experimental Y-parameter evolutions versus the frequency. And when we plot the value of the capacitances obtained $(C_{\rm in}, C_{\rm bc}, C_{\rm out})$ versus the inverse square root

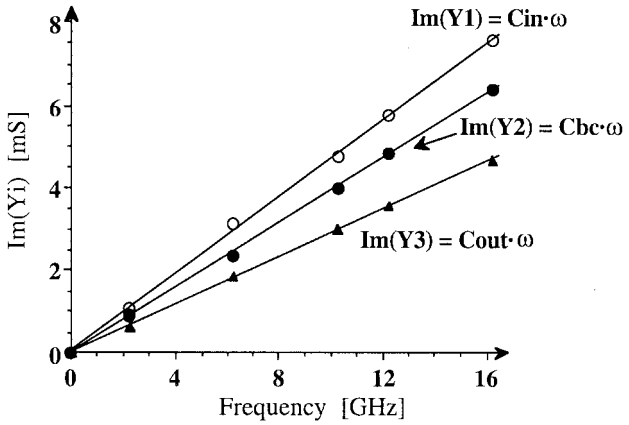

Fig. 4. Typical evolution of the imaginary part of the Y-parameters, when the HBT is reverse-biased, as a function of frequency.

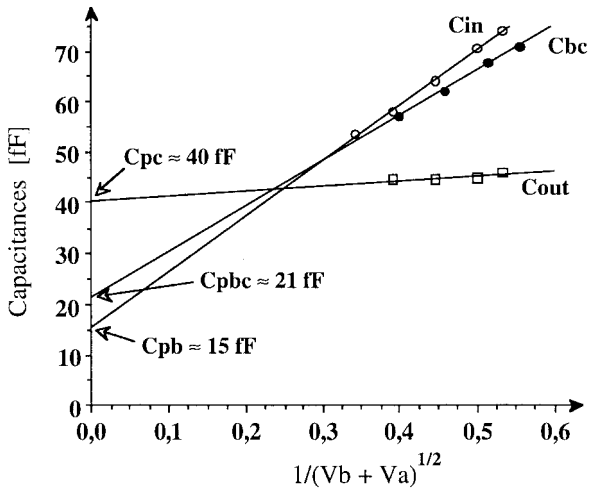

Fig. 5. Typical evolution of the measured capacitances $\{C_{\rm in}, C_{\rm bc}, C_{\rm out}\}$ versus the inverse square root of the applied potential.

TABLE I
EXPERIMENTAL EVOLUTION OF THE CAPACITANCE $C_{\rm ce}$ AS A FUNCTION OF THE APPLIED POTENTIAL

Circuit Element	Vb = 0 V	Vb = - 1 V	Vb = -2 V
Cce (fF)	6	5	5

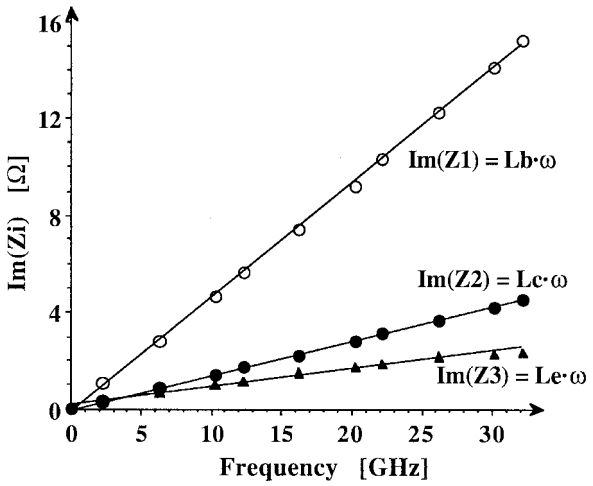

Fig. 6. Typical evolution of the imaginary part of the Z-parameters, when the HBT is forward-biased, as a function of frequency.

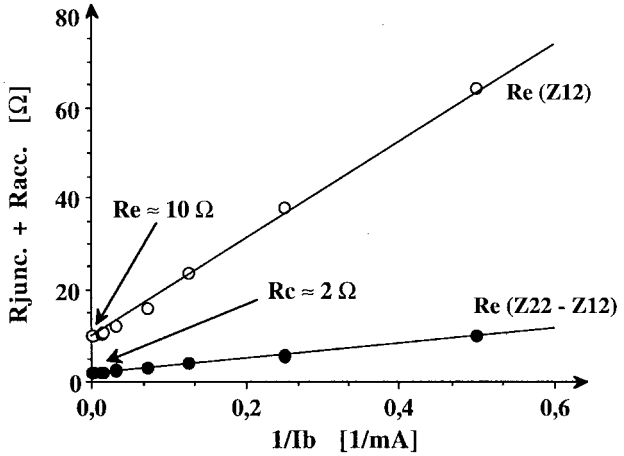

Fig. 7. Plots of the real part of Z_{12} and $\{Z_{22} - Z_{12}\}$ versus $1/I_b$.

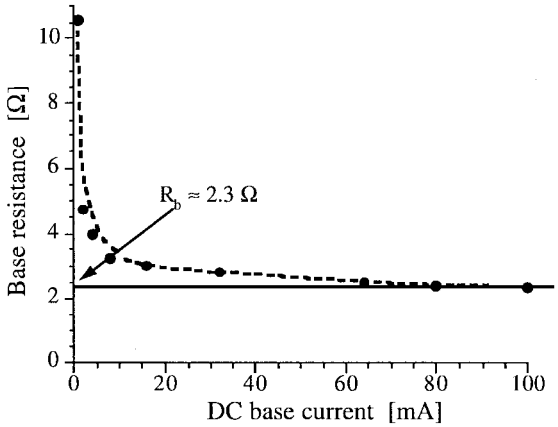

Fig. 8. Typical evolution of the real part of $\{Z_{11} - Z_{12}\} \approx R_{\rm base}$ as a function of the dc base current.

of the applied voltage (Fig. 5), we obtained a linear curve in perfect agreement with the theoretical previsions [see (2)], validating our approach and enabling the extraction of the parasitic capacitances by extrapolation.

We noticed that the output capacitance given by the ratio $C_{\rm out}$ appears also to be slightly bias dependent (Fig. 5), implying the existence of a intrinsic capacitance $C_{\rm ce}$ between the collector and

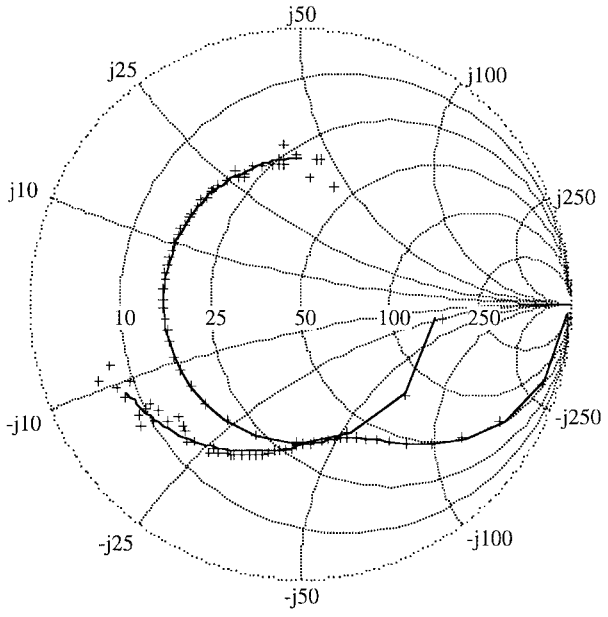

(a)

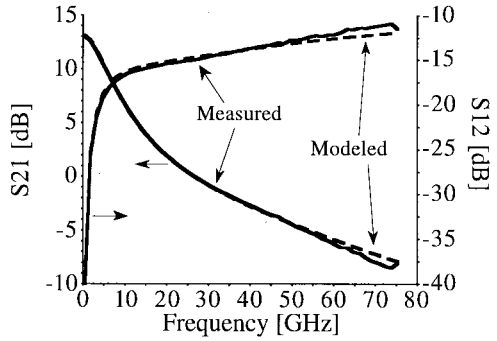

(b)

Fig. 9. Comparison between the measured and the calculated S-parameters of an HBT $\{I_b = 1$ mA, $I_c = 9.4$ mA and $V_{\rm ce} = 2.5$ V$\}$ in the frequency range from 0.25 to 75 GHz (with or without capacitance in parallel with $R_{\rm bi}$).

the emitter, confirming other published suggestions [4]. Since the value of this capacitance $C_{\rm ce}$ is quite small (see Table I), however, the circuit can be simplified by adding it directly to the value of $C_{\rm pc}$, at least in the case of small-signal applications.

B. Parasitic Inductances

To get the value of the parasitic inductances, we also used the method described by Dambrine [1] for the FET or for HBT's by Maas [6]. Indeed, as for the FET, when the HBT is forward-biased and especially for high base–current densities, the influence of the parasitic capacitances remains negligible in comparison with the inductances. Moreover, the junction resistance values tend to zero and the junction capacitances (C_e, C_c and C_j), thus quite large, become a short-circuit past a few hundred megahertz so that the intrinsic Z-matrix (see Fig. 2) cancels. That way, the HBT equivalent circuit may be modeled by a simple T-circuit with its Z-matrix $\{Z_{ij}\}$ written as follows [see (3)]:

$$\begin{aligned} Z_{11} &= Z_1 + Z_2 & Z_1 &= R_b + j\cdot\omega\cdot L_b \\ Z_{12} &= Z_{21} = Z_2 \quad \text{with} & Z_2 &= R_e + j\cdot\omega\cdot L_e \\ Z_{22} &= Z_2 + Z_3 & Z_3 &= R_c + j\cdot\omega\cdot L_c. \end{aligned} \tag{3}$$

Fig. 6 shows the evolution of the imaginary part of the Z-parameters of the HBT when forward-biased, indicating excellent agreement

TABLE II
SURVEY OF THE PARASITIC ELEMENT VALUES OBTAINED THROUGH OUR METHOD. COMPARISON WITH THOSE OBTAINED THROUGH A TEST STRUCTURE AND THE ONE WE OBTAINED AFTER FIT

Circuit Element	Fitted Value	Test Structure	Extracted Val.
L_b (pH)	80		70
L_c (pH)	30		25
L_e (pH)	7		10
C_{pb} (fF)	16.8	19	15
C_{pc} (fF)	42	19	40
C_{pbc} (fF)	16	2.5	21
R_b (Ω)	2.55		2.3
R_c (Ω)	2.5		2
R_e (Ω)	10.5		10
β_o	9.35		9.4
τ (ps)	1.9		
R_{be} (Ω)	27.5		25-30
C_e (pF)	1.85		
R_{bc} (kΩ)	32		
C_c (fF)	13.5		16
C_j (fF)	20		16
R_{bb} (Ω)	8.65		
R_{bi} (Ω)	5.5		
C_{bi} (pF)	6.1		
C_{ce} (fF)	6		5

between the theoretical predictions [see (3)] and the experimental results, thus validating this extraction method.

C. Access Resistances

As for the inductances, we used the techniques proposed by Dambrine [1] and Maas [6] to extract the access resistances. So, to determine the access resistances $(R_{\rm base}, R_e, R_c)$, we have solely to study the evolution of the real part Z-parameters versus $\frac{1}{I_b}\{I_b$: dc base–current through the junction involved$\}$. Indeed, the linear extrapolation of the plot $\mathrm{Real}(Z_{12})$ and $\mathrm{Real}(Z_{22}-Z_{12})$ versus $\frac{1}{I_b}$ to the ordinate gives us the values of R_e and R_c respectively (Fig. 7). However, the determination of the base-resistance is complicated by the fact that beneath the base, there is a distributed diode between the base and the collector that short-circuits the base (Fig. 1). This effect becomes all the more dominant as the forward base–collector current increases, so that the extraction of the entire base–resistance is impossible by using the above method. For high base–current densities, however, it appears that the value of the base resistance leads to a constant value (Fig. 8) related to an extrinsic part of the base resistance, called in our circuit R_b (Fig. 2).

III. EXTRACTION OF INTRINSIC CIRCUIT

After extracting the parasitics, we performed measurements for the HBT in an active bias condition, over a wide frequency range as already stated. In addition, we tested the different intrinsic topologies commonly used (T and π-topology) to finally establish which one effectively works well.

So, throughout this part of our study, we always found a good agreement between the measured and fitted S-parameters by using our equivalent circuit as depicted on Fig. 9, thus validating our circuit and extraction method of the parasitics. An interesting point is that this agreement was always obtained whatever the topology considered (T or π), and that the insensitivity of the fitted values to their starting value was independent of the topology considered. It was also found that the values of the parasitic elements determined after optimization were always in close agreement to those obtained from the extraction using the previously discussed approach (Table II).

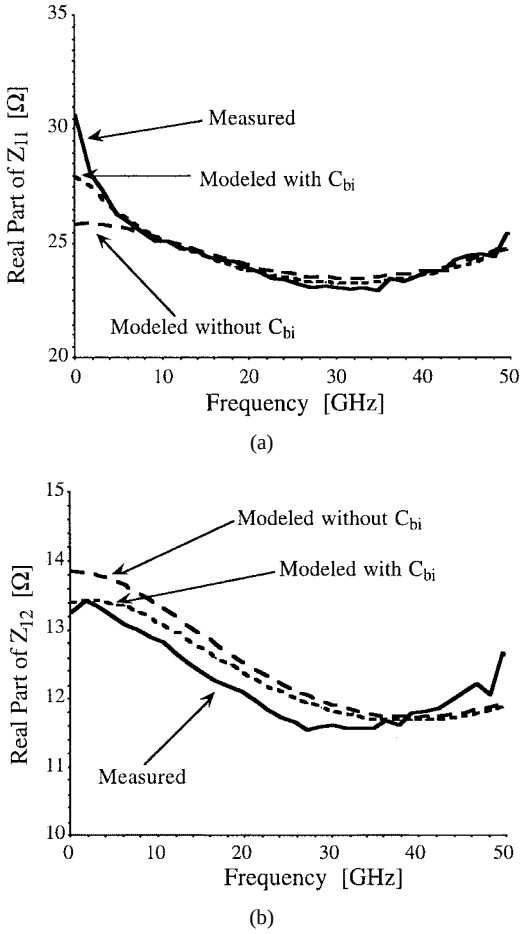

Fig. 10. Comparison between the measured and the calculated parameters, Z_{11} and Z_{12}, of an HBT ($I_b = 1$ mA, $I_c = 9.4$ mA, $V_{\rm ce} = 2.5$ V) with and without capacitance in parallel with $R_{\rm bi}$.

However, although we always had a good agreement between the measured and fitted S-parameters, by studying the Z-matrix, we still observed that Z_{11} and Z_{12} remained incorrectly fitted at low frequencies. This suggested that all or a part of the whole base resistance $\{R_{\rm bi}, R_{\rm bb}$, and $R_b\}$ is short circuited by a capacitance, that is to say that a parallel RC circuit occurs along the base [2]. Finally, we found that by introducing a capacitance in parallel with $R_{\rm bi}$, we obtained the best fit of Z_{11} and Z_{12} for all frequencies (Fig. 10). This capacitance has a quite large value (Table II) (a few picofarads when normally biased, several hundred femtofarads when reverse-biased), which remains difficult to explain.

IV. CONCLUSION

We established that the method using a test structure to extract the parasitics, more particularly the parasitic capacitances, is inaccurate, while the direct extraction method that we propose is a lot more suitable to exactly extract the values of the parasitics. This extraction method validates also our equivalent circuit since a good agreement between the theory and the experiment is obtained for all bias conditions. The values of either the parasitics, once extracted, and the elements that can be assessed through the theory such as

$R_{be}, \beta(\alpha, G_m)$, once the collector and the base–currents are known, remain really close to the fitted ones.

ACKNOWLEDGMENT

The authors acknowledge Siemens for processing the MOVPE-wafers for this work.

REFERENCES

[1] G. Dambrine, A. Cappy, F. Heliodore, and E. Playez, "A new method for determining the FET small-signal equivalent circuit," *IEEE Trans. Microwave Theory Tech.*, vol. 36, July 1988.

[2] D. Costa, W. U. Liu, and J. S. Harris, "Direct extraction of the AlGaAs/GaAs heterojunction bipolar transistor small-signal equivalent circuit," *IEEE Trans. Electron Devices*, vol. 38, Sept. 1991.

[3] R. A. Pucel and U. L. Rohde, "An exact expression for the noise resistance R_n for the Hawkins bipolar noise model," *IEEE Microwave Guided Wave Lett.*, vol. 3, Feb. 1993.

[4] S. Maas, B. L. Nelson, and D. L. Tait, "Intermodulation in heterojunction bipolar transistors," *IEEE Trans. Microwave Theory Tech.*, vol. 40, Mar. 1992.

[5] U. Schaper, K. H. Bachem, M. Karner, and P. Zwicknagl, "Scaling of small-signal equivalent circuit elements for GaInP/GaAs hole-barrier-bipolar-transistors," *IEEE Trans. Electron Devices*, vol. 40, Jan. 1993.

[6] S. A. Maas and D. Tait, "Parameter-extraction method for heterojunction bipolar transistors," *IEEE Microwave Guided Wave Lett.*, vol. 2, Dec. 1992.

[7] S. Lee and A. Gopinath, "Parameter extraction technique for HBT equivalent circuit cutoff mode measurement," *IEEE Trans. Microwave Theory Tech.*, vol. 40, Mar. 1992.

[8] D. R. Pehlke and D. Pavlidis, "Evaluation of the factors determining HBT high-frequency performance by direct analysis of S-parameter data," *IEEE Trans. Microwave Theory Tech.*, vol. 40, Dec. 1992.

A Rigorous Analysis of a Cross Waveguide to Large Circular Waveguide Junction and Its Application in Waveguide Filter Design

Ke-Li Wu and Robert H. MacPhie

***Abstract*—A rigorous analysis is obtained for the problem of scattering at the junction of a cross-shaped waveguide and a larger circular waveguide. The general case of an arbitrary offset and orientation of the cross waveguide axes is considered. The fields matching over the cross aperture of the smaller guide is facilitated by using the transformation of the circular cylindrical Bessel–Fourier modal fields of the circular guide into a finite series of exponential plane wave functions. This permits an analytical finite series solution for the elements of the fields mode matching matrix, from which the general scattering matrix of the junction is obtained. The application of the formulation to circular waveguide filter design is emphasized in the numerical examples. Excellent agreements between theoretical and experimental results are obtained in all the numerical examples.**

***Index Terms*—Modal analysis, waveguide filter design, waveguide junction.**

Manuscript received November 10, 1995. This work was supported in part by the Natural Sciences and Engineering Research Council of Canada.

K.-L. Wu is with Corporate Research and Development Department, COM DEV Ltd., Cambridge, ON N1R 7H5, Canada.

R. H. MacPhie is with Department of Electrical and Computer Engineering, University of Waterloo, Waterloo, ON N2L 3G1, Canada.

Publisher Item Identifier S 0018-9480(97)00431-6.

I. INTRODUCTION

Due to the significant position of narrow bandwidth multimode channel filters in communication satellite payloads [1], rigorous electromagnetic (EM) modeling of the filters has become an urgent task since the circuit theory model [2] was developed by Atia and Williams in the 1970's. An accurate modeling and design of the channel filters will considerably reduce or even hopefully eliminate the manual tuning process. One of the key elements in the EM filter design is the modeling of cross- or rectangular-shaped irises between circular waveguide cavities.

Because of the difficulties engendered by the different geometrical coordinates in the iris aperture and circular waveguides (one is rectangular, another is circular), analysis of these types of junctions has shown that "there appears to be no easy analytical solution" [3] and numerical integration has been used [3]–[5].

Fortunately, an easy analytical solution has been available using a plane-wave finite series expansion of the Bessel–Fourier modal eigenfunction in the circular waveguide [6]. An analytical solution for the scattering of smaller rectangular-to-circular waveguides has been given in [6]. This paper will provide a rigorous analysis of an arbitrary offset and orientation cross waveguide to a large circular waveguide junction. Applications of the analysis to waveguide filter design will be emphasized. This is an extension of the work in [6] to a more practical case in waveguide dual mode filter design.

Instead of treating the horizontal and vertical slots separately, as in [4], the cross-shaped slot will be treated as a complete waveguide. The advantages of the new formulation over previous works are: 1) it provides the coupling information for a slot in one direction in the presence of another slot in the perpendicular direction; 2) the coupling information for both slots can be obtained at same time, which is very important in full EM analysis of circular waveguide dual mode filters; and 3) full analytical expressions to be deduced for the elements of the modal analysis matrix equation lead to a rigorous and efficient solution of the problem.

The formulation has been verified by experiments and excellent agreements are obtained.

II. THEORY

A. Mode Functions in Cross Waveguide

The generalized crossed rectangular waveguide considered in this paper is depicted in Fig. 1(a). The modes in the cross waveguide are grouped according to their symmetry with respect to the x and y axis. The modal solutions have been discussed in [7]. For clarity, the nth mode functions for each group will be summarized in the following compact form:

$$\vec{e}_{ht1}{}^{n} = -N_h^n \sum_r \Phi_{1r}^n \{\left(\frac{r\pi}{2d}\right) Q[p_{1r}^n(\frac{x}{2a}-\frac{1}{2})]P[\frac{r\pi(d-y)}{2d}]\hat{x} - \left(\frac{p_{1r}^n}{2a}\right) R[p_{1r}^n(\frac{x}{2a}-\frac{1}{2})]\cdot S[\frac{r\pi(d-y)}{2d}]\hat{y}\} \tag{1a}$$

$$\vec{e}_{et1}{}^{n} = N_e^n \sum_r \Phi_{1r}^n \{\left(\frac{p_{1r}^n}{2a}\right) Q[p_{1r}^n(\frac{x}{2a}-\frac{1}{2})]P[\frac{r\pi(d-y)}{2d}]\hat{x} - \left(\frac{r\pi}{2d}\right) R[p_{1r}^n(\frac{x}{2a}-\frac{1}{2})]\cdot S[\frac{r\pi(d-y)}{2d}]\hat{y}\} \tag{1b}$$